Supplemental Data.

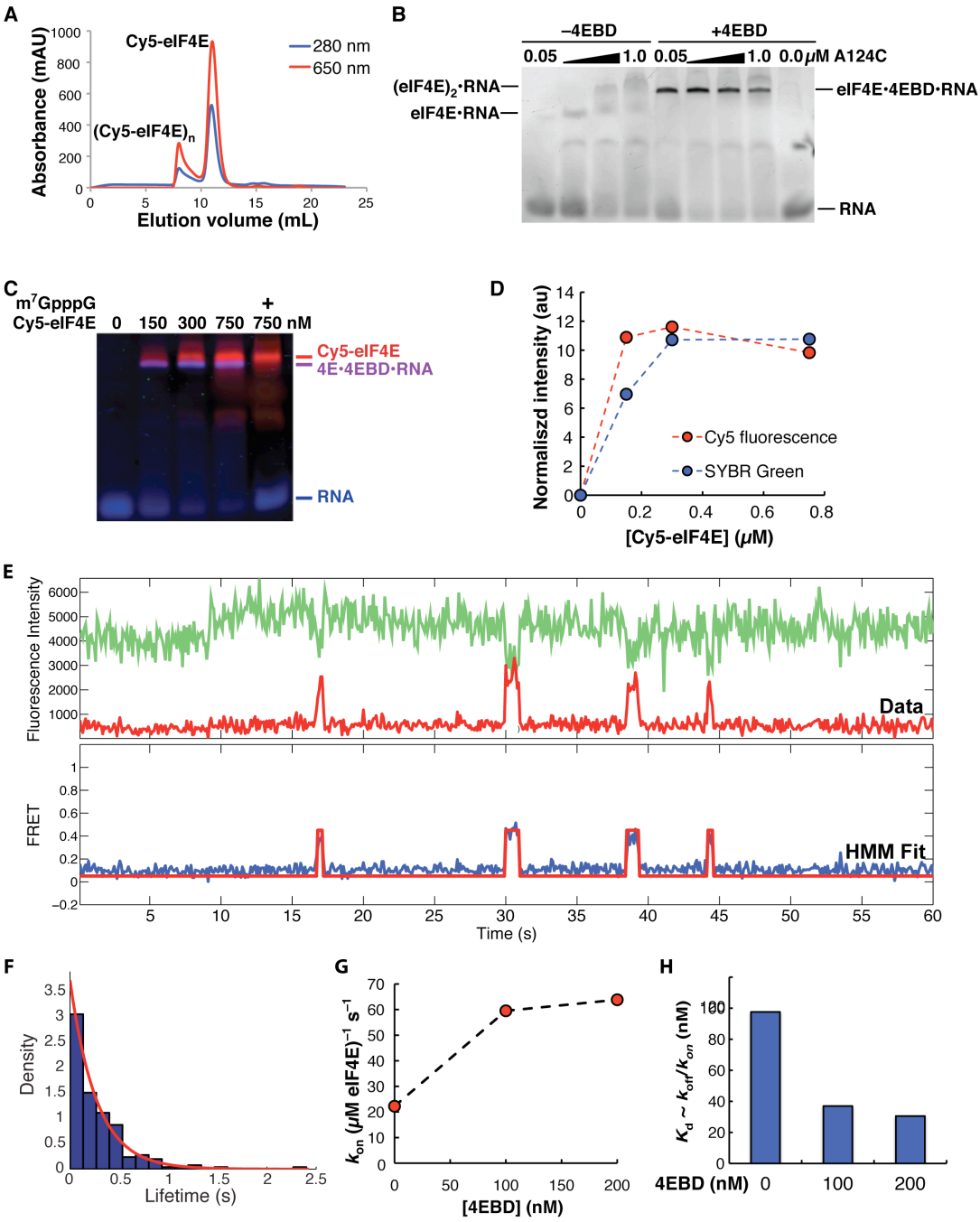

Figure S1. Relates to Figure 1. Preparation and activity of Cy5-eIF4E. (**A**) Size exclusion chromatogram (Superdex 75, 26/60, GE Healthcare) of Cy5-eIF4E. The monomeric protein elutes between 10 and 12 mL, after dimeric and tri-/multimeric protein. The observed A_{650}/A_{280}

ratio indicates a labeling efficiency of 50%. **(B)** Native gel shift assay for binding of eIF4E(A124C) to a capped oligoribonucleotide (m^7GpppGG$(CU)_{10}$GCG$(CGA)_3$) in the absence and presence of eIF4G1-4EBD. The results suggest the formation of protein-RNA complexes with one, two, or three eIF4E molecules in the absence of 4EBD. When 4EBD was present, a single, high-affinity ternary complex was observed. Gels were imaged by staining for RNA using SYBR Green I nucleic acid gel stain (Life Technologies/Invitrogen). **(C)** Gel shift assay for binding of Cy5-eIF4E to the model capped RNA, imaged using Cy5 fluorescence and RNA staining. **(D)** Densitometric quantitation of the formation of the Cy5-eIF4E•4EBD•RNA ternary complex in panel (C). **(E)** Representative single-molecule trace showing HMM fit for binding of 7.5 nM Cy5-eIF4E to surface-immobilized, capped poly(CU) RNA. **(F)** Representative FRET lifetime distribution for the Cy5-eIF4E•poly(CU) complex, with single-exponential fit. **(G)** Association rates measured by single-molecule FRET, and **(H)** calculated dissociation constants (k_{off}/k_{on}) for the Cy5-eIF4E•4EBD•RNA ternary complex with polyhistidine-tag-free Cy5-eIF4E.

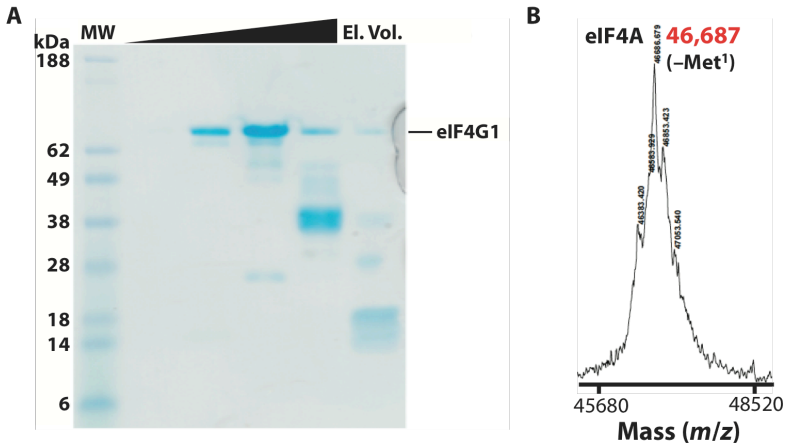

Figure S2. Relates to Figure 2. Purification of polyhistidine-tagged eIF4G1 and eIF4A. **(A)** SDS-PAGE analysis of fractions from Superdex 200 (26/60) purification of eIF4G1. The highest molecular weight fractions, in the leftmost analytical lane, were used in single-molecule studies. Protein identity was confirmed by MALDI-TOF mass mapping. **(B)** MALDI-TOF mass spectrum of purified recombinant His_6-eIF4A. The isolated protein lacks the *N*-terminal methionine (Calc.: 46,712, Obs.: 46,687).

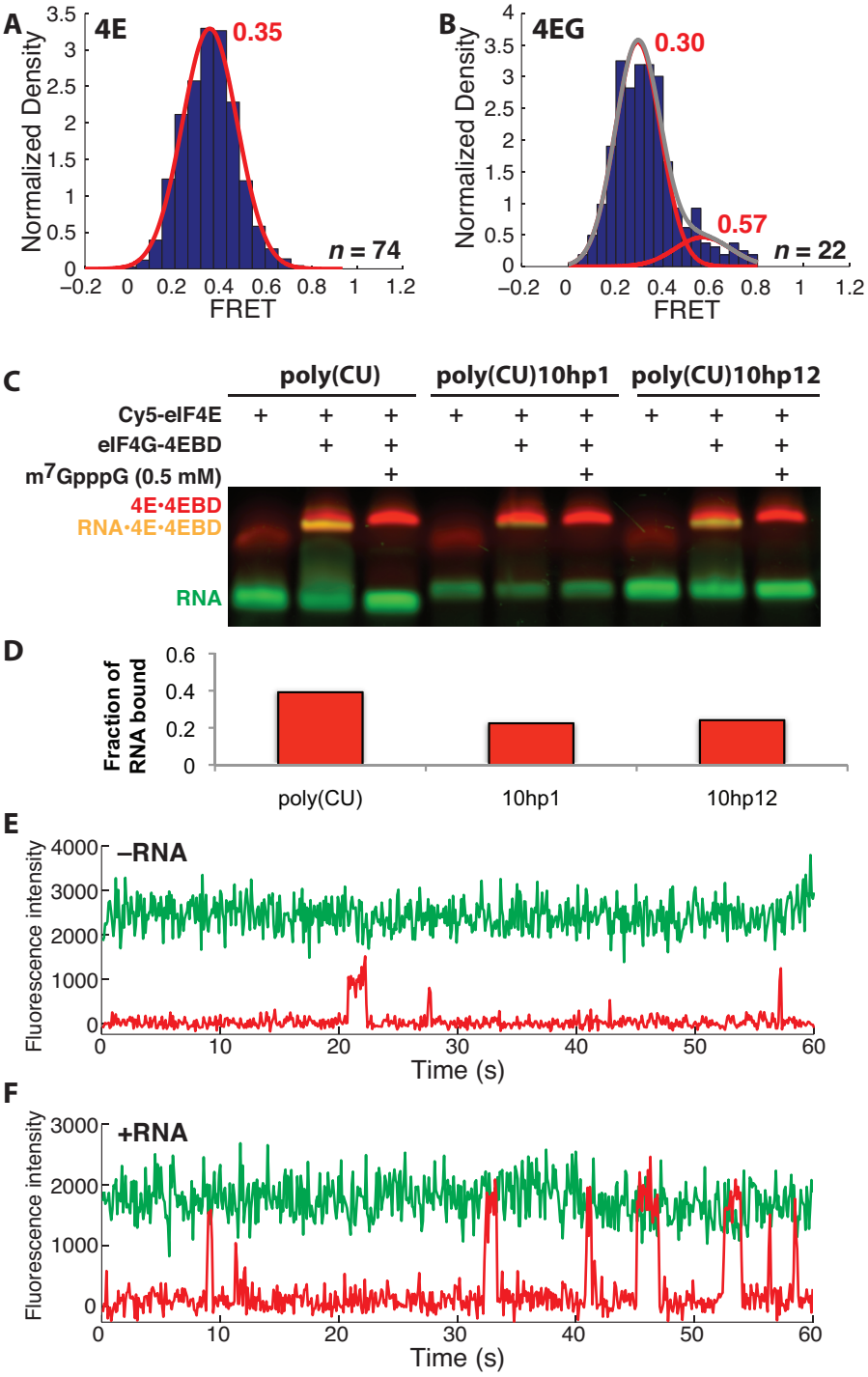

Figure S3. Relates to Figure 3. Binding of Cy5-eIF4E to poly(CU)10hp RNAs. **(A)** FRET distribution for the Cy5-eIF4E•poly(CU)10hp12 complex. **(B)** FRET distribution for the Cy5-eIF4E•eIF4G1•poly(CU)10hp12 complex. **(C)** Binding of 200 nM Cy5-eIF4E to poly(CU) and

poly(CU)10hp RNAs (50 nM, poly(CU) and 10hp12; ~25 nM, 10hp1) in the presence of 5 μM eIF4G-4EBD, assayed by native gel shift. **(D)** Densitometric quantitation of the fraction of each RNA in (C) bound in the Cy5-eIF4E•4EBD•Cy3-RNA complex. **(E)** Representative trace from green-red illumination experiment showing non-specific Cy5-eIF4E events at a surface lacking RNA. Cy5-eIF4E was present at 7.5 nM. **(F)** Representative trace from dual green-red illumination experiment as in panel (D), but with immobilized poly(CU)10hp1, showing additional Cy5 events due to binding of Cy5-eIF4E to the immobilized RNA. The number of single-molecule traces (*n*) used to construct histograms is given for each distribution.

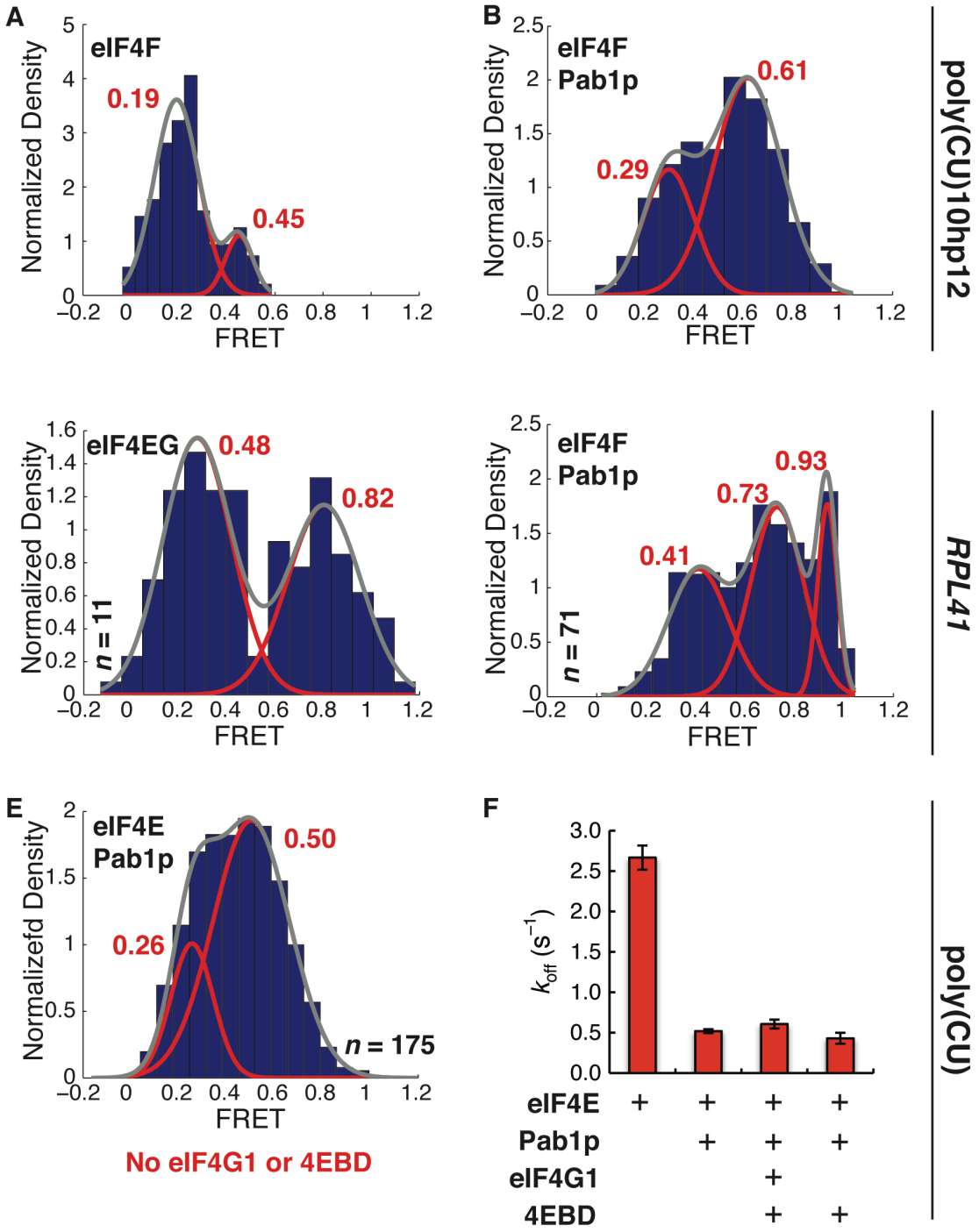

Figure S4.

Figure S4. Relates to Figure 4. Effect of Pab1p on FRET distributions for eIF4E•RNA complexes. **(A)** FRET distribution for the Cy5-eIF4E•eIF4G1•eIF4A•cap-poly(CU)10hp12 complex, fit to a double Gaussian distribution. **(B)** FRET distribution for the Cy5-

eIF4E•eIF4G1•eIF4A•Pab1p•cap-poly(CU)10hp12 complex, fit to a double Gaussian distribution. **(C)** FRET distribution for the Cy5-eIF4E•eIF4G1•cap-*RPL41* complex, fit to a double Gaussian distribution. **(D)** FRET distribution for the Cy5-eIF4E•eIF4G1•eIF4A•Pab1p•cap-*RPL41* complex, fit to a triple Gaussian distribution. **(E)** FRET distribution for the Cy5-eIF4E•Pab1p•cap-poly(CU) complex, lacking eIF4G1 or eIF4G-4EBD, fit to a double Gaussian distribution. **(F)** Observed rate of dissociation of the Cy5-eIF4E•cap-poly(CU) complex in the presence of Pab1p (2 μM), eIF4G1 (250 nM), and eIF4G-4EBD (250 nM). The increased lifetime associated with the presence of Pab1p is observed regardless of the presence of eIF4G1/4EBD. Error bars reflect standard errors from a single-exponential fit to lifetime distributions. The number of single-molecule traces (*n*) used to construct histograms is given for each distribution.

Supplemental Experimental Procedures.

Plasmid construction.

Standard molecular biology techniques were used. The *CDC33* gene encoding eIF4E was PCR-amplified from yeast genomic DNA using a forward primer that introduced a 5′ NdeI site followed by a sequence encoding a TEV protease cleavage site, and a reverse primer that introduced a 3′ KpnI site. The PCR product was purified, digested, ligated into similarly-digested pET-28a(+). The A124C mutation was then introduced by QuikChange site-directed mutagenesis (Agilent Technologies).

The fragment of *TIF4631* encoding the eIF4G1 4E-binding domain and flanking sequences, the *TIF2* gene encoding eIF4A, and the *PAB1* gene encoding Pab1p, were also PCR-amplified from yeast genomic DNA using appropriate primers and ligated into pET-28a(+).

Full-length, *N*-terminally polyhistidine-tagged eIF4G1 was co-expressed with eIF4E using the pETDuet-1 vector. The *TIF4631* coding sequence was placed in multiple cloning site (MCS) 1, while the *CDC33* coding sequence was placed in MCS 2.

Expression strains.

Gene	**Protein**	**Vector**	**5′/3′ sites**	***E. coli* host**
CDC33	eIF4E	pET-28a(+)	NdeI/KpnI	BL21 Star (DE3)
TIF4631	eIF4G-4EBD	pET-28a(+)	NcoI/XhoI	BL21 Star (DE3)
TIF4631	eIF4G1	pETDuet-1 (MCS1)	BamHI/HindIII	BL21(DE3) RIG
TIF2	eIF4A2	pET-28a(+)	NdeI/XhoI	BL21(DE3)
PAB1	Pab1p	pET-28a(+)	NcoI/XhoI	BL21(DE3)

Protein purification.

For eIF4E, eIF4G-4EBD, and eIF4A, the lysis buffer was 50 mM HEPES-KOH, pH 7.4, 300 mM KCl, 20 mM imidazole, 2.5 mM TCEP. The lysate was clarified by centrifugation (14,500 rpm, 25 minutes), and the clarified lysate was filtered through a 0.2 μm syringe filter, then applied to 1.5 mL Ni^{2+}-NTA agarose. The column was washed with 50 mL of the same buffer containing 50 mM imidazole, then eluted with buffer containing 250 mM imidazole. The imidazole was removed by gel filtration using an Econo-Pac 10 DG desalting column (Bio-Rad). The resulting protein solution was concentrated to ~700 μL and applied to a HiLoad 26/60 Superdex 75 preparative grade column (GE Healthcare Life Sciences) equilibrated in 50 mM HEPES-KOH, pH 7.4, 300 mM KCl, 2.5 mM DTT. Fractions of eluate containing the most pure eIF4E were pooled. The concentration of these pooled fractions was typically 5–10 μM; this protein solution was used without further processing. Attempts to freeze the protein for long-

term storage consistently resulted in its inactivation; we therefore prepared and labeled the protein every 2–3 weeks, which we found to be the time scale on which it retains high levels of activity when stored at 6 ˚C.

The majority of experiments were carried out with the polyhistidine-tagged protein; removal of the tag had no detectable effect on the binding dynamics of the Cy5-eIF4E•4EBD complex (Figure S1E). The polyhistidine tag was removed with AcTEV Protease (Invitrogen) using the manufacturer's protocol and an overnight incubation at 6 ˚C.

For full-length eIF4G1, the purification was as described above, but the buffers contained 1.0 M KCl and 2.5 mM $MgCl_2$. Even under these high-salt conditions, the protein co-purified with significant quantities of RNA, observed from the A_{260}/A_{280} ratio of the protein as it eluted from the size exclusion column. A HiLoad 26/60 Superdex 200 preparative grade column (GE Healthcare Life Sciences) was used for size exclusion purification of full-length eIF4G1.

The identity of purified proteins was confirmed by mass spectrometry. eIF4E, eIF4G-4EBD, and eIF4A were analyzed by MALDI-TOF MS. In the case of His_6-eIF4G1, the molecular ion for the full-length, polyhistidine-tagged protein could not be detected (Calc.: 108,502 Da); instead an ion of mass 103,575 Da was observed that is consistent with a truncation encompassing residues 34 to 952 (out of 952). Analysis of the purified protein by peptide mass mapping of a sample excised from an SDS-PAGE gel confirmed the presence of peptides that encompassed residues 15 to 741. The data thus suggest that our preparation of eIF4G1 contains the full-length protein or at worst the ΔN15 protein. Peptide mass mapping was also used to confirm the identity of Pab1p.